

Article

Effect of Injection Flow Rate on Product Gas Quality in Underground Coal Gasification (UCG) Based on Laboratory Scale Experiment: Development of Co-Axial UCG System

Akihiro Hamanaka ^{1,*}, Fa-qiang Su ^{2,3}, Ken-ichi Itakura ^{3,4}, Kazuhiro Takahashi ^{3,4}, Jun-ichi Kodama ⁵ and Gota Deguchi ⁶

¹ Department of Earth Resources Engineering, Kyushu University, 744 Motooka, Nishi-ku, Fukuoka 819-0395, Japan

² School of Energy Science and Engineering, Henan Polytechnic University, 2001 Century Avenue, Jiaozuo 454-003, Henan, China; sfqmuroran@gmail.com

³ Center of Environmental Science and Disaster Mitigation for Advanced Research, Muroran Institute of Technology, 27-1 Mizumoto, Muroran 050-8585, Japan; itakura@mmm.muroran-it.ac.jp (K.I.); ktakahashi@mmm.muroran-it.ac.jp (K.T.)

⁴ Department of Information and Electronic Engineering, Muroran Institute of Technology, 27-1 Mizumoto, Muroran 050-8585, Japan

⁵ Division of Sustainable Resources Engineering, Hokkaido University, Kita 13 Nishi 8, Kita-ku, Sapporo 060-8628, Japan; kodama@eng.hokudai.ac.jp

⁶ Underground Resources Innovation Network, Kita 47 Higashi 17, Higashi-ku, Sapporo 007-0847, Japan; gota@mue.biglobe.ne.jp

* Correspondence: hamanaka@mine.kyushu-u.ac.jp; Tel.: +81-92-802-3331

Academic Editor: Mehrdad Massoudi

Received: 7 January 2017; Accepted: 13 February 2017; Published: 16 February 2017

Abstract: Underground coal gasification (UCG) is a technique to recover coal energy without mining by converting coal into a valuable gas. Model UCG experiments on a laboratory scale were carried out under a low flow rate (6~12 L/min) and a high flow rate (15~30 L/min) with a constant oxygen concentration. During the experiments, the coal temperature was higher and the fracturing events were more active under the high flow rate. Additionally, the gasification efficiency, which means the conversion efficiency of the gasified coal to the product gas, was 71.22% in the low flow rate and 82.42% in the high flow rate. These results suggest that the energy recovery rate with the UCG process can be improved by the increase of the reaction temperature and the promotion of the gasification area.

Keywords: underground coal gasification; gasification efficiency; co-axial UCG system; acoustic emission

1. Introduction

Underground coal gasification (UCG) is a technique to extract energy from coal in the form of heat energy and combustible gases through chemical reactions in the underground gasifier. The product gas has as a variety of uses: electricity supply with a gas turbine, hydrogen production, and the other chemical feedstock [1–4]. UCG technology enables us to utilize coal resources that remain unrecoverable underground due to either technological or economic reasons. The annual consumption of coal in Japan was 177 million tons in 2014 while the annual domestic coal production is only 1.3 million tons [5]. This fact means that more than 99% of the coal used in Japan depends on importation from overseas countries. Additionally, 25% of the domestic primary energy supply consists of coal. Now, Japan has an underground and several surface coal mines in a limited region.

Actually, the geological conditions of the coal seam in Japan are quite complicated as it has many faults, foldings, and steep dipping. Accordingly, most coal mines had to be closed because of the difficulty of mining, high operation costs, and high labor costs. However, abundant unused coal resources remain underground. Such coal resources are estimated to be 30 billion tons. For that reason, UCG has great potential to recover vast amounts of energy from these coal resources.

Many benefits are anticipated from this technology: utilizing unused coal, lower capital/operating costs, no surface disposal ash, and the possibility of the combination of carbon capture and storage. In the UCG process, the oxidants are injected from an injection well in order to promote the gasification reactions, and product gas consists of CO, H₂, CH₄, CO₂, and other hydrocarbons are recovered from a production well. Typical reaction zones during the UCG process can be divided roughly into three zones [6]: The oxidation zone, the reduction zone, and the drying and pyrolysis zone (Figure 1). Oxidation is source of heat to promote the gasification process, meaning that the oxidation reaction makes the temperature of the coal seam rise. Reduction is the main chemical reaction in the UCG process. In this process, CO₂ or H₂O_(g) are reduced to CO and H₂ as the main chemical reactions. As these reactions are endothermic reactions, the temperature of the coal seam is decreased when promoting the reduction reactions. On the other hand, these chemical reactions are promoted under high temperatures. In summary, one of keys to success in an efficient UCG process is to keep a high temperature in the reaction zone. In the drying and pyrolysis zone, various kinds of gases are formed, not only CH₄, CO, CO₂, H₂, but also other hydrocarbons.

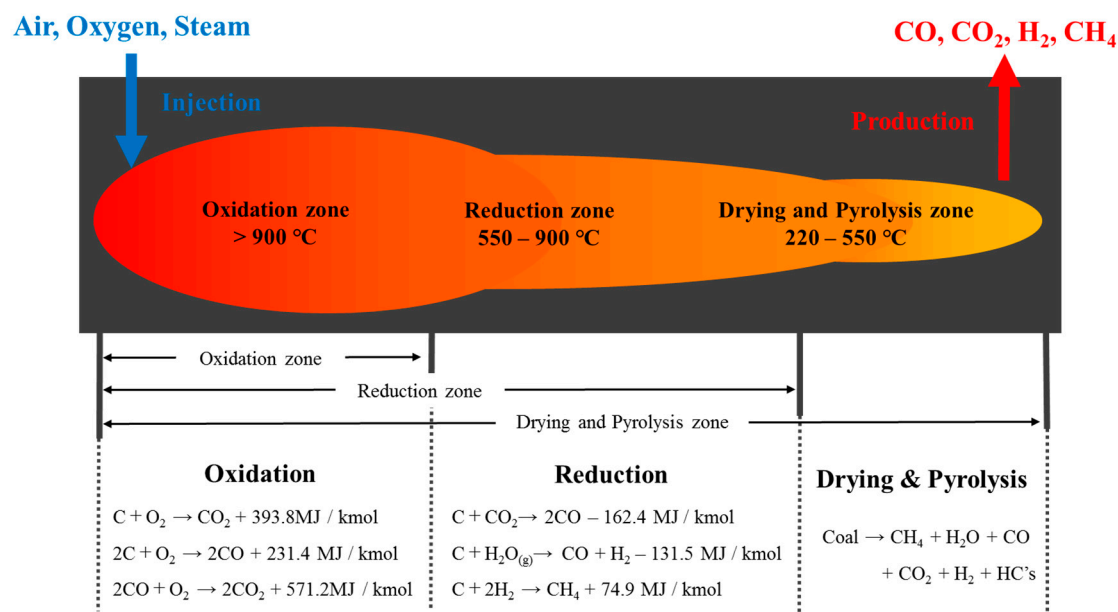


Figure 1. Typical chemical reaction zone during UCG process.

The contents of the product gas can be roughly controlled with the temperature and the injection materials in the surface coal gasification plant. It is, however, difficult to control the quality of the product gas during the UCG process because the conditions of the underground reactor are constantly changing due to changes in the temperature field and the expansion of the cavity [7,8]. The composition of the product gas changes depending on the injected oxidant used, the operating pressure, the coal quality, and the mass and energy balance of the underground reactor [9]. The calorific value of the product gas recovered by UCG is usually low (3–4 MJ/Nm³) when air is injected as a gasification agent, meaning that the usage of the gas is limited because of its low calorific value. On the other hand, researchers have obtained results to improve the quality of the product gas by using a mixture of air and oxygen due to an increase of the reaction temperature in the underground reactor [10–12].

We discuss the development of a co-axial UCG system, which is compact and flexible, that can be adopted under complicated geological conditions [13–15]. A co-axial UCG system uses only one well set with a double pipe: oxidants are injected from an inner pipe, and product gases generated in the coal seam are collected from an outer pipe (Figure 2). This UCG system has superiority in terms of applicability compared to the conventional one, but the recovered energy from the coal is relatively low because the gasification area in a co-axial system is limited around a well even though operating this system saves costs [16,17].

From these backgrounds, the objective of this study is to clarify the effect of the injection flow conditions on the product gas quality including the gasification efficiency, which means the conversion efficiency of the gasified coal (chemical energy of product gas/chemical energy of gasified coal), in order to develop a co-axial UCG system with high efficiency.

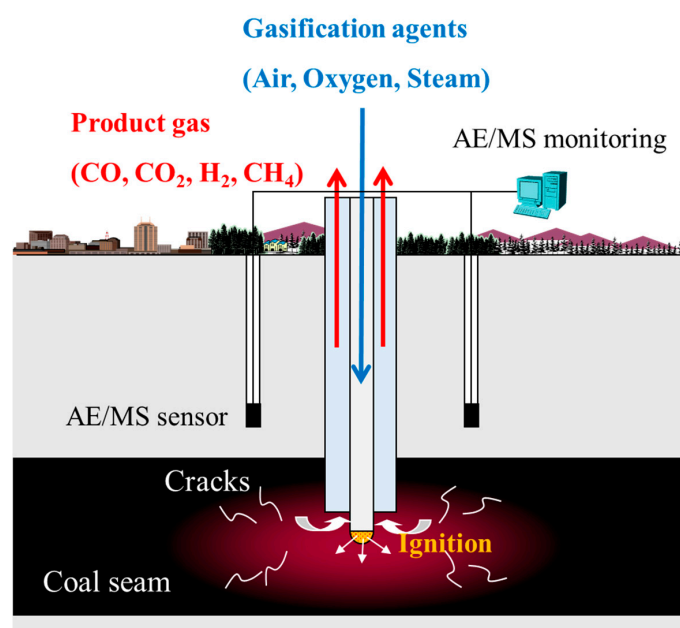


Figure 2. Concept of co-axial UCG system.

2. Materials and Methods

A diagram of model UCG experiment conducted using a coal block is shown in Figure 3. The coal blocks used in this study were rectangular shape that the range of length and width are 0.15~0.20 m, and the range of height is 0.20~0.25 m. Coal samples were supplied from Sanbi Mining Co., Ltd., Hokkaido, Japan. Typical proximate and ultimate analyses of the coal are shown in Table 1.

The samples were put into a drum can which had 0.28 diameter and 0.36 m height. The space between them was filled by heat-resistant cement in order to prevent heat release and gas leakage. A co-axial well which is used for ignition, and production well was prepared with 35 mm diameter. Ignited charcoals were supplied to the bottom of a co-axial well in an ignition stage, then a mixture of air and oxygen was supplied continuously as a gasification agent in order to sustain the gasification process. In this study, the model UCG experiments were carried out under the different flow rate to estimate the effects of injection flow, the lower flow rate (experiment 1: 6~12 L/min) and the higher flow rate (experiment 2: 15~30 L/min), on the quality of product gas while the oxygen concentration was kept as stable (50%) based on the previous experiments [14]. During the gasification process, the injection flow rate was arranged to keep the optimal thermodynamic conditions for gasification reactions. Figure 4 shows the injection conditions applied for each experiment. At the end of these experiments, CO₂ or N₂ gas which turned down coal temperature was injected to extinguish the combustion. The total times to inject gasification agents in respective experiments were almost 7 h.

After the process, a mixture of white cement and gypsum was filled into the post-gasification cavity to investigate the gasification area by means of a cross-section study.

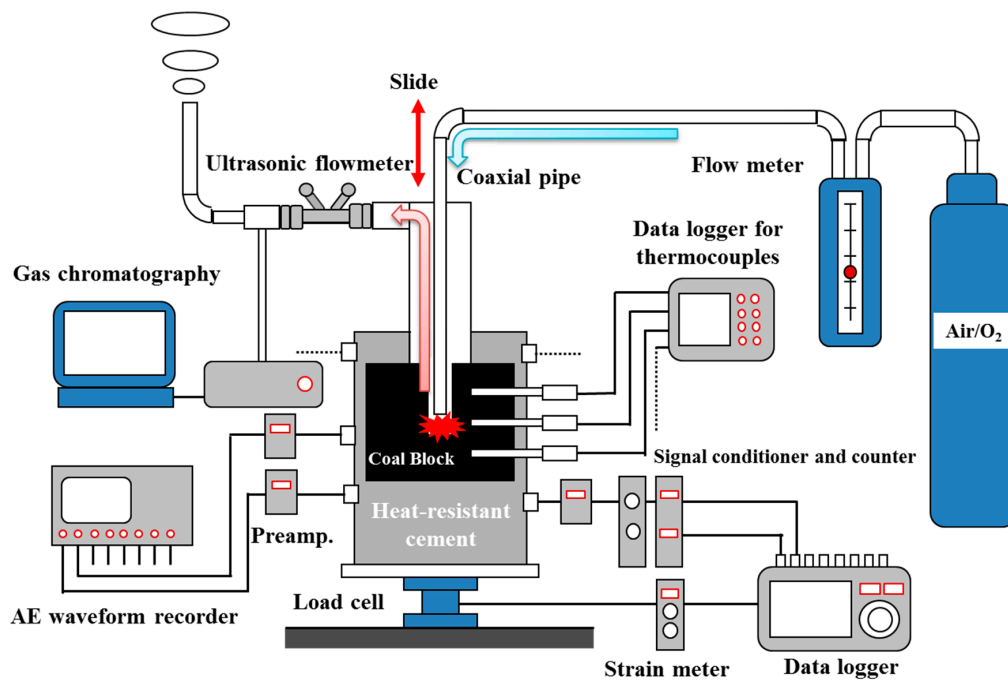


Figure 3. A diagram of the UCG model experiment.

Table 1. Proximate and ultimate analyses of the coal.

Calorific Value (MJ/kg)	Proximate Analysis (wt. %)				Ultimate Analysis (wt. %)				
	Moisture	Ash	Volatiles	Fixed Carbon	C	H	N	S	O
31.48	1.1	8.1	44.9	45.9	75.0	5.78	1.23	0.07	9.71

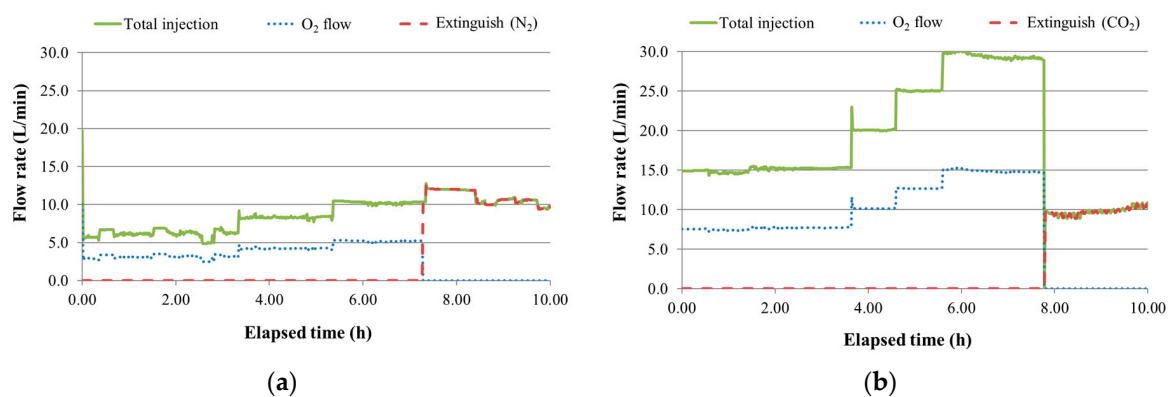


Figure 4. Gasification agents during experiments: (a) Experiment 1; (b) Experiment 2.

The flow rate of the product gas was measured using an ultrasonic flowmeter. The compositions of product gas (O_2 , N_2 , CO_2 , H_2 , CO , CH_4 , C_2H_4 , C_2H_6 , C_3H_6 , and C_3H_8) were monitored every 30 min using a gas chromatograph (Micro GC 3000A; INFICON Co., Ltd., East Syracuse, NY, USA). Meanwhile, temperature and acoustic emission (AE) were monitored to visualize inner part of the coal sample and obtain the data about fracturing activities by using type K thermocouples (SUS310S; Chino Corp., Tokyo, Japan) and piezoelectric acceleration transducers (620 HT; TEAC Corp., Tokyo, Japan), respectively. The layout of sensors are shown Figure 5.

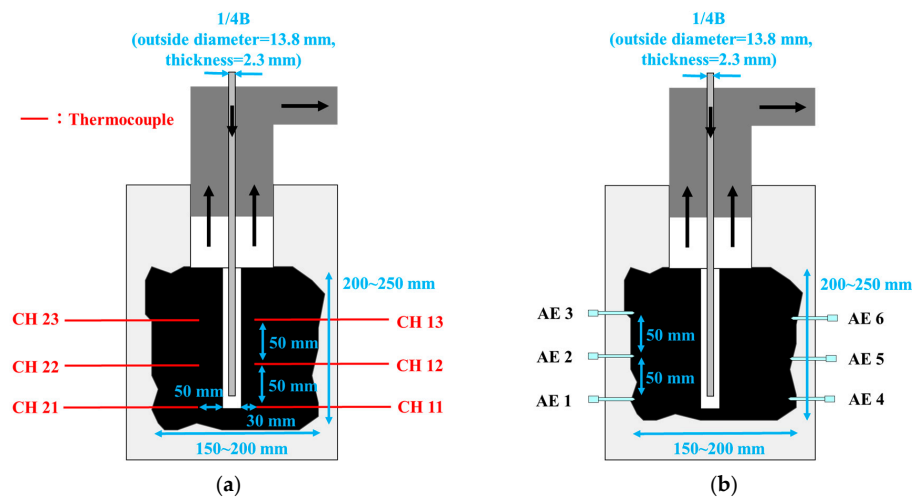


Figure 5. Layout of sensors: (a) Thermocouples; (b) Piezoelectric acceleration transducers.

AE is a kind of phenomenon to emit low-level elastic wave from solids when they are stressed or deformed. The number of AE occurrences are commonly increased just before solids is destructed: the stress of rock reach to uniaxial compressive strength in uniaxial compressive test. AE monitoring is, therefore, used in the field of rock mechanics, concrete, and mining to predict the damage and the failure of brittle materials because they reach structural failure by accumulating microfracture [18–22]. As many AE activities can be detected attributable to thermal stress during UCG process [23], it is also useful to estimate the progress of gasification process and special events such as collapse of coal in the cavity and extensive propagation of gasification zone. In this study, AE events and AE counts are calculated by means of data processing of the raw AE signal data, as shown in Figure 6. Both parameters are counted when AE signal is higher than a threshold. Besides, AE event is not counted until the signal is damped. The dead time meaning for that period is usually several milliseconds in brittle materials: rock, concrete, and coal. AE events show the number of cracks initiated inside a coal sample and AE counts reflect the magnitude of AE event. All AE waveforms from the sensors were recorded using an oscilloscope (GR-7000; Keyence Corp., Elmwood Park, NJ, USA) with sampling time of 10 μ s.

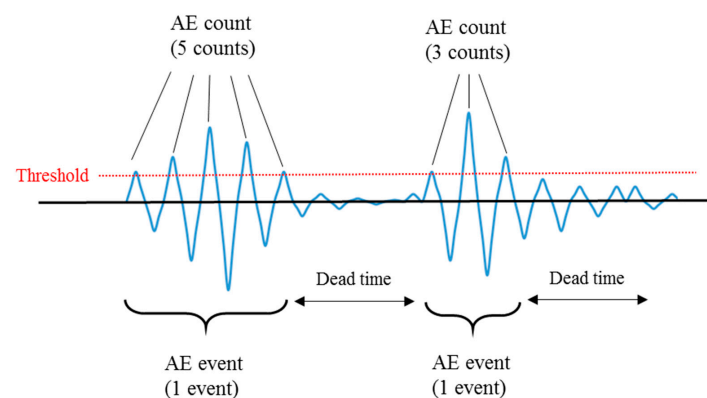


Figure 6. Definition of AE event and AE count.

3. Results and Discussion

3.1. Temperature and AE

Temperature profiles for each experiment are plotted against the elapsed time in Figure 7. The trend of the temperature increment was almost the same in both experiments. The temperatures

in T11 and T12 located in the lower part of the co-axial well increased in the initial stage of the experiment. Subsequently, the temperatures increased in T13, T21, and T22. These results indicate that the gasification area moved in an upward direction along the co-axial well and expanded to the wider area. Regarding the temperature increment quantity, the maximum coal temperature in experiment 2 reached over 1200 °C, much higher than that in experiment 1. Besides, the high temperature area expanded quickly in experiment 2. These results can be explained by the promotion of the oxidation reaction with the increase of the oxygen inflow because the coal temperature increased with the oxidation reaction and reacted with the coal and oxygen. This finding leads to a possibility to create a larger gasification area with a higher temperature for a short period of time due to the promotion of the oxidation reaction.

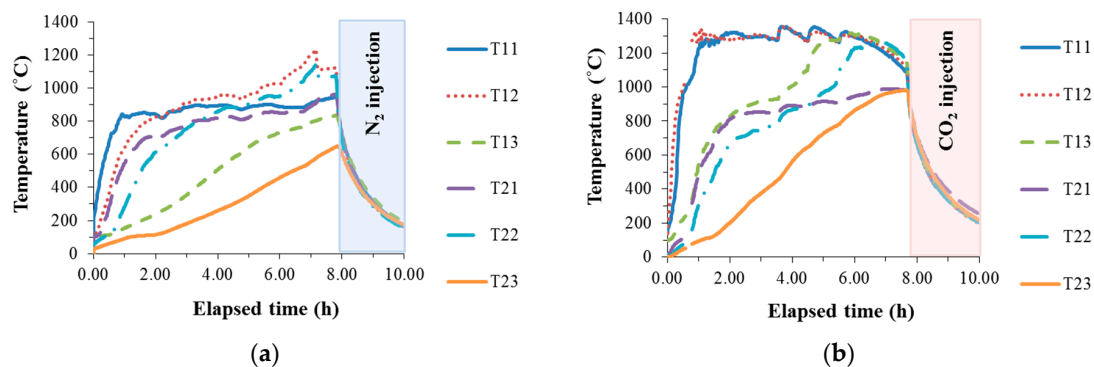


Figure 7. Temperature profiles: (a) Experiment 1; (b) Experiment 2.

Figure 8 shows the results of AE activities for each experiment. From the results of the AE event, it increased with the elapsed time in both experiments, meaning that the number of the fracturing events increased. Based on the results of the temperature profile, we can consider that the fracturing events are generated in a wide range due to the expansion of the gasification zone in the later stage of the experiments. Additionally, AE events in the initial stage of experiment 2 were higher than those of experiment 1 and the AE counts were the highest in the initial stage of experiment 2, when the temperature changed drastically. This means that the fracturing events caused by the thermal stress were activated in experiment 2 after the ignition of the coal. The activation of fracturing events creates a large number of cracks; as a result, chemical reactions are promoted and are attributable to increasing the reaction-specific surface area. Therefore, the reaction area of coal gasification can be expanded by utilizing thermal stress leading to activated fracture events under the high temperature.

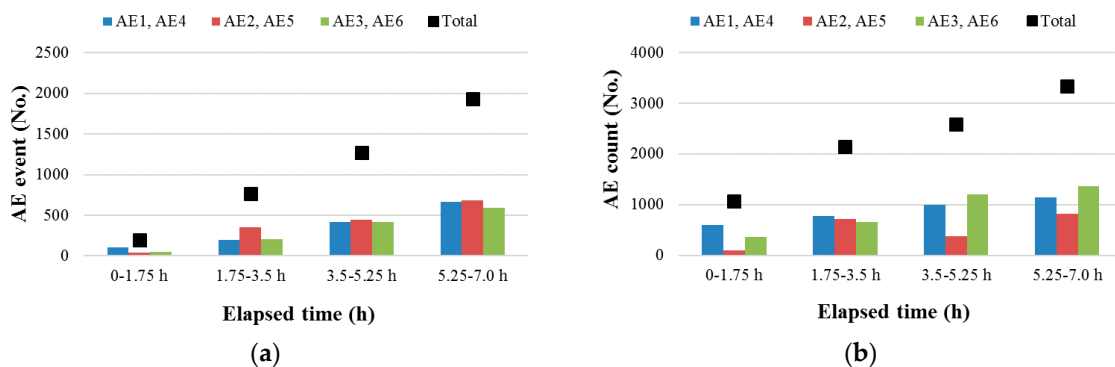


Figure 8. Cont.

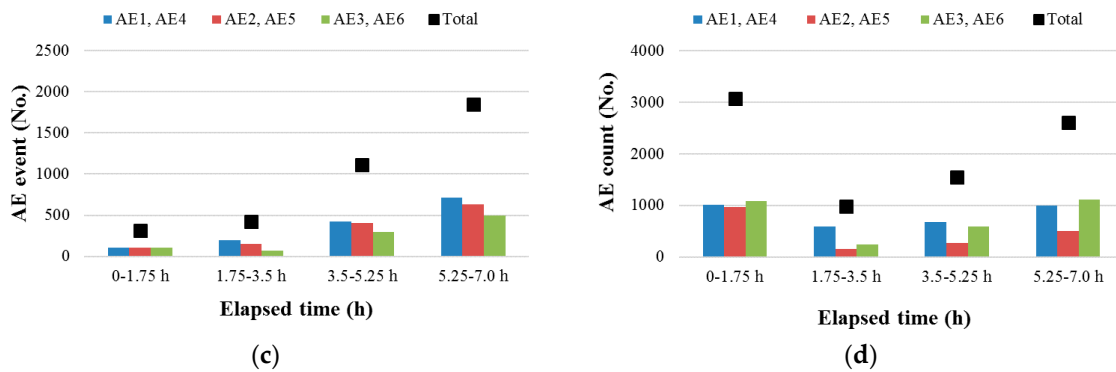


Figure 8. Monitoring results of AE activities: (a) AE events (experiment 1); (b) AE counts (experiment 1); (c) AE events (experiment 2); (d) AE counts (experiment 2).

3.2. Product Gas Quality and Gasification Efficiency

Figure 9 shows the monitoring results of the main compositions and the calorific value of the product gas, which can be calculated with the concentration of the combustible gas contents such as CO, CH₄, H₂, and other hydrocarbons [24]. The calorific value of the product gas in experiment 2 decreased dramatically with a decrease of the combustible gas contents after 2 h elapsed, while that of experiment 1 decreased slightly. These differences are attributed to the inhibition of the gasification reaction with the heat-resistant cement around a coal block based on the results of a cross-section study after the experiment (Figure 10), meaning that the gasification area expanded rapidly in the initial stage due to the excess oxygen inflow in experiment 2. Additionally, the calorific value in the end phase of experiment 1 was relatively lower than that in the beginning of experiment 2 even though the injection flow rate was somewhat similar. Molten slag was generated during the gasification process due to the ash contents of the coal. Therefore, the slag formation may prevent the promotion of the gasification reaction because of the limitation of the gas-solid contact. From these considerations, the effect of the injection flow rate on the quality of the product gas and the gasification efficiency, which means the energy recovery rate from coal, is discussed by using a part of the data which were not affected by the heat-resistant cement and the slag formation. The range of data processing was 0.5~3.0 h for experiment 1, and 0.5~1.5 h for experiment 2. The flow rate in these ranges for both experiments was stable (6 L/min for experiment 1, 15 L/min for experiment 2). Additionally, the total amount of oxygen inflow was almost the same in these ranges.

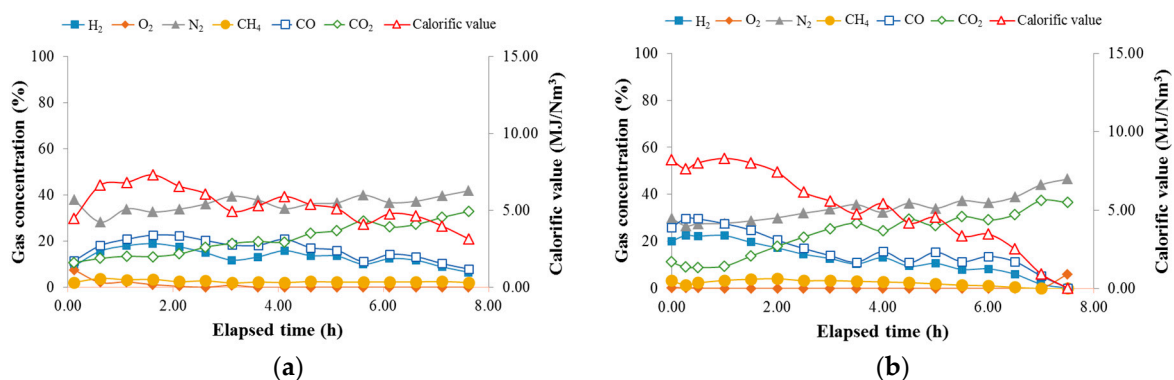


Figure 9. Main compositions and the calorific value of a product gas: (a) Experiment 1; (b) Experiment 2.

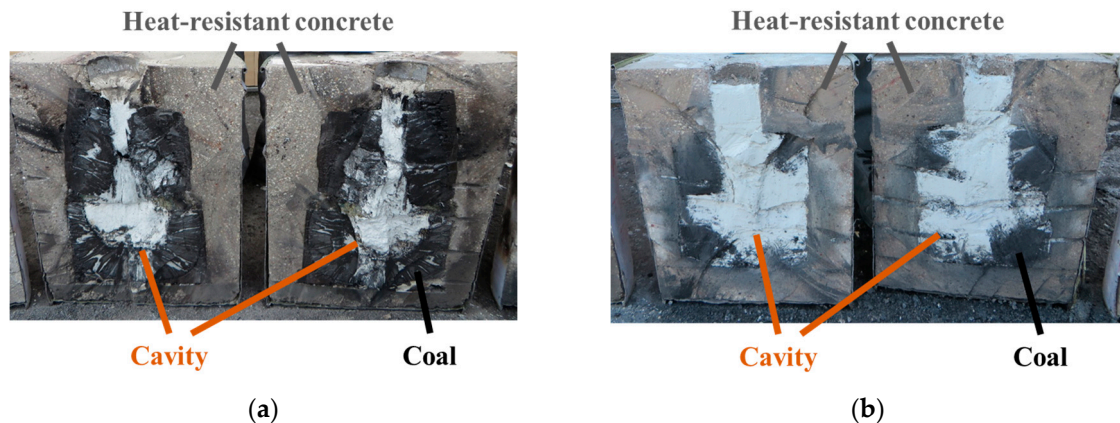


Figure 10. Cross-section study after the experiment: (a) Experiment 1; (b) Experiment 2.

The typical product gas data in the range of data processing are listed in Table 2. The average calorific value and the total production flow of the product gas in experiment 2 were higher than those in experiment 1. These differences can be explained by the promotion of the reduction reaction in which combustible gas contents were produced during the UCG process because the concentrations of H_2 and CO were higher, and that of CO_2 was lower in experiment 2. This fact indicates that the gasification reactions are promoted under high temperature in the gasification regions as a result of the increase of the oxygen inflow to activate the oxidation reaction.

Table 2. Typical product gas data (0.5~3.0 h for experiment 1, 0.5~1.5 h for experiment 2).

	Average Calorific Value (MJ/Nm ³)	Total Product Flow (m ³)	N ₂ , O ₂ Free			
			H ₂ (%)	CH ₄ (%)	CO (%)	CO ₂ (%)
Experiment 1	6.39	1.57	29.34	5.40	38.20	22.11
Experiment 2	8.11	2.26	33.65	5.19	45.23	17.61

Balance computation is a useful method to discuss the amount of coal reacted in the UCG process [25]. The amount of gasified coal is calculable by the balance of the C element, as shown in Table 3. The amount of carbon content in a tar is not included in the balance sheet. The amounts of C reacted in experiments 1 and 2, respectively, were 0.37 kg and 0.57 kg, meaning that 0.50 kg and 0.76 kg of coal are expected to have been gasified based on the ultimate analyses of the coal. Considering that the coal calorific value was 31.48 MJ/kg, the gasification efficiency, the energy recovery rate from coal, is calculable using Equation (1).

$$R_g = \frac{E_T / W_g}{Q_c} \times 100, \quad (1)$$

where R_g is the gasification efficiency (%), E_T means the total energy (MJ), W_g represents the gasified coal (kg), and Q_c stands for the coal calorific value (MJ/kg).

Table 3. Calculation of C balance (0.5~3.0 h for experiment 1, 0.5~1.5 h for experiment 2).

Component	Experiment 1			Experiment 2		
	Total Amount of Product Gas	Balance of C Element		Total Amount of Product Gas	Balance of C Element	
	mol	mol	kg	mol	mol	kg
CH ₄	2.32	2.32	0.03	3.64	3.64	0.04
CO	15.87	15.87	0.19	30.11	30.11	0.36
CO ₂	11.45	11.45	0.14	11.82	11.82	0.14
C ₂ H ₄	0.49	0.98	0.01	0.84	1.68	0.02
C ₂ H ₆	0.12	0.24	0	0.15	0.30	0.00
C ₃ H ₆	0.06	0.18	0	0.00	0.00	0.00
C ₃ H ₈	0.02	0.06	0	0.00	0.00	0.00
Total	30.33	31.1	0.37	46.56	47.55	0.57

Table 4 presents the calculation results for the gasification efficiency. The energy of the product gas can be calculated with the product flow rate and the calorific value of the product gas. The values for the gasification efficiency in experiments 1 and 2, respectively, are 71.22% and 82.42%. A comparison of the results shows that the UCG process with the higher oxygen inflow has a higher efficiency for energy recovery from coal than that with the lower oxygen inflow, attributable to increasing the combustible contents in the product gas. The product gas quality depends on the reduction reaction during the UCG process, meaning that the temperature field is strongly affected. Therefore, it might be possible to estimate the gasification efficiency by creating a proper numerical model. Additionally, it is pointed out that the recovered energy from coal can be improved with the increase of the reaction temperature and the expansion of the gasification area during the UCG process. In summary, an increase of the oxygen inflow makes the temperature of the coal increase by the promotion of the oxidation reaction; then the fracture events are activated. As a result, the quality of the product gas is improved, attributable to expanding the gasification area with a high temperature.

Table 4. Calculation of gasification efficiency (0.5~3.0 h for experiment 1, 0.5~1.5 h for experiment 2).

	Coal Calorific Value (MJ/kg)	Energy of Product Gas (MJ)	Amount of C Element (kg)	Gasified Coal (kg)	Gasification Efficiency (%)
Experiment 1	31.48	11.21	0.37	0.50	71.22
Experiment 2		19.72	0.57	0.76	82.42

The product gas recovered with the UCG process is variable depending on the type of UCG operation, the coal quality, and the underground conditions. According to the results of this study, a key factor to improve the quality of the product gas is to expand the gasification reaction area with an increase of the reaction temperature. The reaction temperature can be improved by the promotion of the oxidation reaction while the expansion of the reaction area depends on the coal characteristics. It means that not only injection conditions but also the improvement of the gasifier conditions to promote the expansion of reaction area should be discussed to develop a highly efficient UCG system.

4. Conclusions

The injection condition is one of the key parameters to control the product gas quality in the UCG process. This paper discussed the effect of the injection flow rate on the product gas quality by means of model UCG experiments on a laboratory scale. The results showed that the gasification efficiency can be improved with the increase of the reaction temperature and the expansion of the gasification area by increasing the oxygen inflow. This finding suggests that a key issue for the improvement of the gasification efficiency is to control the gasifier conditions. The proper injection conditions promote

the oxidation reaction which increases the coal temperature, leading to activation of fracturing events caused by thermal stress. Therefore, the control of fracturing events is another option that can be considered for the improvement of the overall process.

To develop a more efficient UCG system, the improvement techniques to expand the gasification area with a high temperature, such as the improvement of coal permeability and the effects of the reactor pressure, are necessary to investigate in future studies.

Acknowledgments: This work was supported by the Japanese Society on UCG, Mikasa City, Center of Environmental Science and Disaster Mitigation for Advanced Research of Muroran Institute of Technology, JSPS KAKENHI Grant Number 15H02332, Sanbi Mining Co., Ltd., the Ministry of Education, Culture, Sports, Science and Technology (MEXT), Japan. The authors gratefully acknowledge their support.

Author Contributions: A.H. and K.I. conceived and designed the experiments; F.S. performed the experiments; K.T. carried out gas analysis and analyzed the data; J.K. and G.D. extensively supported to the experiments and the data analyses with constructive advises; A.H. wrote the paper.

Conflicts of Interest: The authors declare no conflict of interest.

References

1. Khadse, A.; Qayyumi, M.; Mahajani, S.; Aghalayam, P. Underground coal gasification: A new clean coal utilization technique for India. *Energy* **2007**, *32*, 2061–2071. [CrossRef]
2. Porada, S.; Czerski, G.; Dziok, T.; Grzywacz, P.; Makowska, D. Kinetics of steam gasification of bituminous coals in terms of their use for underground coal gasification. *Fuel Process. Technol.* **2015**, *130*, 282–291. [CrossRef]
3. Stańczyk, K.; Kapusta, K.; Wiatowski, M.; Świadrowski, J.; Smoliński, A.; Rogut, J.; Kotyrba, A. Experimental simulation of hard coal underground gasification for hydrogen production. *Fuel* **2012**, *91*, 40–50. [CrossRef]
4. Yang, L.H.; Zhang, X.; Liu, S.Q.; Yu, L.; Zhang, W.L. Field test of large-scale hydrogen manufacturing from underground coal gasification (UCG). *Int. J. Hydrogen Energy* **2008**, *33*, 1275–1285. [CrossRef]
5. Japan's Energy White Paper 2016. Available online: http://www.enecho.meti.go.jp/about/whitepaper/2016pdf/whitepaper2016pdf_2_1.pdf (accessed on 28 December 2016).
6. Yang, L.; Liang, J.; Yu, L. Clean coal technology—Study on the pilot project experiment of underground coal gasification. *Energy* **2013**, *28*, 1445–1460. [CrossRef]
7. Nourozieh, H.; Kariznovi, M.; Chen, Z.; Abedi, J. Simulation Study of Underground Coal Gasification in Alberta Reservoirs: Geological Structure and Process Modeling. *Energy Fuels* **2010**, *24*, 3540–3550. [CrossRef]
8. Luo, Y.; Coertzen, M.; Dumble, S. Comparison of UCG cavity growth with CFD model predictions. In Proceedings of the Seventh International Conference on CFD in the Minerals and Process Industries, Melbourne, Australia, 9–11 September 2009.
9. Bhutto, A.W.; Bazmi, A.A.; Zahedi, G. Underground coal gasification: From fundamental to applications. *Prog. Energy Combust. Sci.* **2013**, *39*, 189–214. [CrossRef]
10. Kačur, J.; Durdán, M.; Laciak, M.; Flegner, P. Impact analysis of the oxidant in the process of underground coal gasification. *Measurement* **2014**, *51*, 147–155. [CrossRef]
11. Stańczyk, K.; Howaniec, N.; Smoliński, A.; Świadrowski, J.; Kapusta, K.; Wiatowski, M.; Grabowski, J.; Rogut, J. Gasification of lignite and hard coal with air and oxygen enriched air in a pilot scale ex situ reactor for underground gasification. *Fuel* **2011**, *90*, 1953–1962. [CrossRef]
12. Hongtao, L.; Feng, C.; Xia, P.; Kai, Y.; Shuqin, L. Method of oxygen-enriched two-stage underground coal gasification. *Min. Sci. Technol. (China)* **2011**, *21*, 191–196. [CrossRef]
13. Su, F.Q.; Itakura, K.; Deguchi, G.; Ohga, K.; Goto, T. Laboratory Studies on Evaluation of Gasification Effect for Conversion of Coal Resources in Underground Coal Gasification (UCG) reactors. *Adv. Mater. Res.* **2012**, *600*, 111–115. [CrossRef]
14. Su, F.Q.; Itakura, K.; Hamanaka, A.; Deguchi, G.; Ohga, K. Ex-situ UCG Model Experiments with Oxygen Enriched Air in an Artificial Coal Seam. In Proceedings of the International Conference on Material Science and Engineering Technology 2016, Phuket, Thailand, 14–16 October 2016.
15. Su, F.Q.; Itakura, K.; Hamanaka, A.; Deguchi, G.; Ohga, K. Evaluation of gasification zone and energy recovery during UCG process with the Coaxial models. In Proceedings of the 5th Sustainable Energy and Environmental Sciences, Singapore, 22–23 February 2016.

16. Hamanaka, A.; Itakura, K.; Su, F.Q.; Takahashi, K.; Satoh, K.; Deguchi, G.; Kodama, J. Model Experiment for Co-axial Underground Coal Gasification System Development. In Proceedings of the 24th World Mining Congress (Sustainability in Mining), Rio de Janeiro, Brazil, 18–21 October 2016.
17. Hamanaka, A.; Itakura, K.; Su, F.Q.; Satoh, K.; Takahashi, K.; Deguchi, G.; Kodama, J.; Ohga, K. Development of Compact Underground Coal Gasification (UCG) System as a Local Energy Resource. In Proceedings of the International Symposium on Earth Science and Technology 2015, Fukuoka, Japan, 3–4 December 2015.
18. Lokner, D. The Role of Acoustic Emission in the Study of Rock Fracture. *Int. J. Rock Mech. Min. Sci. Geomech. Abstr.* **1993**, *30*, 883–899. [[CrossRef](#)]
19. Tang, C.A.; Liu, H.; Lee, P.K.K.; Tsui, Y.; Tham, L.G. Numerical studies of the influence of microstructure on rock failure in uniaxial compression—Part I: Effect of heterogeneity. *Int. J. Rock Mech. Min. Sci.* **2000**, *37*, 555–569. [[CrossRef](#)]
20. Li, Y.P.; Chen, L.Z.; Wang, Y.H. Experimental research on pre-cracked marble under compression. *Int. J. Solids Struct.* **2005**, *42*, 2505–2516. [[CrossRef](#)]
21. Zhang, M.; Shimada, H.; Sasaoka, T.; Matsui, K.; Dou, L. Seismic energy distribution and hazard assessment in underground coal mines using statistical energy analysis. *Int. J. Rock Mech. Min. Sci.* **2013**, *64*, 192–200. [[CrossRef](#)]
22. Suzuki, T.; Ohtsu, M. Quantitative damage evaluation of structural concrete by a compression test based on AE rate process analysis. *Constr. Build. Mater.* **2004**, *18*, 197–202. [[CrossRef](#)]
23. Su, F.Q.; Nakanowatari, T.; Itakura, K.; Ohga, K.; Deguchi, G. Evaluation of Structural Changes in the Coal Specimen Heating Process and UCG Model Experiments for Developing Efficient UCG Systems. *Energies* **2013**, *6*, 2386–2406. [[CrossRef](#)]
24. Su, F.Q.; Itakura, K.; Deguchi, G.; Ohga, K.; Kaiho, M. Evaluation of Energy Recovery from Laboratory Experiments and Small-scale Field Tests of Underground Coal Gasification (UCG). *J. MMIJ* **2015**, *131*, 203–218. [[CrossRef](#)]
25. Wiatowski, M.; Kapusta, K.; Świadrowski, J.; Cybulski, K.; Ludwik-Pardala, M.; Grabowski, J.; Stańczyk, K. Technological aspects of underground coal gasification in the Experimental “Barbara” Mine. *Fuel* **2015**, *159*, 454–462. [[CrossRef](#)]



© 2017 by the authors; licensee MDPI, Basel, Switzerland. This article is an open access article distributed under the terms and conditions of the Creative Commons Attribution (CC BY) license (<http://creativecommons.org/licenses/by/4.0/>).